Roles of π-Alkyne, Hydride–Alkynyl, and Vinylidene Metal Species in the Conversion of Alkynes into Vinylidene: New Theoretical Insights

Enrique Peréz-Carreño,[a][+] Paola Paoli,[b] Andrea Ienco,[a] and Carlo Mealli*[a]

Keywords: Ab initio calculations / EHMO / Vinylidene complexes / Cobalt / Rhodium

The transformation of acetylene into vinylidene, as promoted by the metal fragment $[(pp_3)Co]^+$ [$pp_3 = P(CH_2CH_2PPh_2)_3$], is unimolecular and features the hydride–acetylide species as an intermediate. The paper describes a detailed ab initio study of the reaction, in particular with regard to the step involving 1,3-H shift. The best computational results are obtained by mimicking the pp_3 ligand with actual ethylenic chains rather than with single PH_3 molecules. The keypoints along the two-step reaction path (π-acetylene, hydride–acetylide, and vinylidene complexes, as well as intermediate transition states) have been optimized for Co^I and Rh^I derivatives at the MP2 level. For the fragment $[(pp_3)Co]^+$, the barrier associated with transformation of the hydride–acetylide intermediate to vinylidene (20.6 kcal/mol) is easier to surmount compared to that for reversion to the reactants (28.6 kcal/mol). The situation is reversed for the analogous Rh^I system, with the initial π-acetylene adduct being slightly more stable. Although higher in energy, the hydride–acetylide species is the experimentally detected product of the reaction of acetylene with the fragment $[(pp_3)Rh]^+$. The salient chemical aspects of the 1,3-H shift are discussed in terms of perturbation theory arguments. Parallel EHMO calculations, which have provided a relatively good consistency with the ab initio results, allow the proposal of an orbital rationale for the mode of migration of the hydride ligand along the substantially linear $Co–C_\alpha–C_\beta$ grouping.

Introduction

The conversion of unsubstituted or monosubstituted acetylene into vinylidene has been widely investigated both experimentally[1] and theoretically.[2] The strongly endothermic reaction $HC{\equiv}CH \rightarrow :C{=}CH_2$ (ca. 45 kcal/mol) becomes more feasible in the presence of numerous ancillary metal fragments. Following the first EHMO studies,[3] the problem of the metal-promoted interconversion has also been tackled by several groups using higher-level ab initio theory.[4] Briefly, we wish to summarize what is known about the reaction **I**, which may follow alternative pathways.

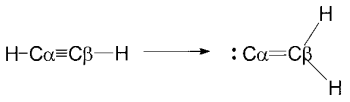

I

The least-motion 1,2-shift seems to be best promoted by d^6 metal fragments, which initially form π-adducts with the alkyne. For example, the early EHMO analysis was consistent with the latter mechanism in the case of $[CpMn(CO)_2]$.[3] More recent ab initio calculations were supportive of the same pathway for the fragment $Cl_2(PH_3)_2Ru$.[4a] There are cases, however, for which the formation of a metal hydride−acetylide species has been documented[5−7] and the question remains open as to whether the latter is the actual intermediate en route to the vinylidene complex (steps *a* and *b* in **II**, correspond to C−H oxidative addition followed by 1,3-H shift) or is merely formed as a side-product. If the latter were to be the case, the formation of vinylidene would also imply the reverse of step *a* (reductive elimination) followed by the 1,2-H shift itself (step *c*).

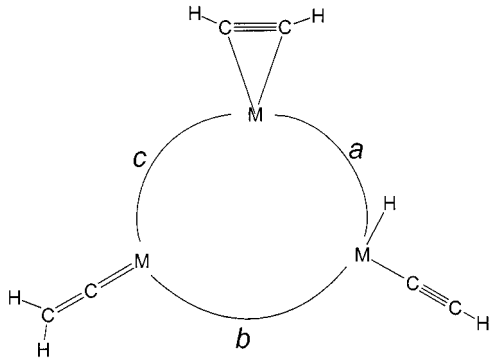

II

This point is still the subject of a passionate debate involving both experimentalists and theoreticians. The situation may vary considerably depending on the nature of the metal fragment. For example, in a recent theoretical study[4c] the possibility that 1−2 tautomerization or hydride−

[a] Istituto per lo Studio della Stereochimica ed Energetica dei Composti di Coordinazione, CNR,
Via J. Nardi 39, I-50132 Firenze, Italy
Fax: (internat.) +39 55 2478366
E-mail: mealli@fi.cnr.it
[b] Dipartimento di Energetica, Università di Firenze,
Via Santa Marta, I-50100 Firenze, Italy
[+] On leave from the Departamento de Química Física y Analítica, Universidad de Oviedo, Spain.

  1434−1948/99/0808−1315 $ 17.50+.50/0

acetylide formation might be involved in acetylene polymerization promoted by electron-deficient metal fragments [e.g. X_4W (X = F, Cl)] was ruled out. On the other hand, Werner et al.[5] reported that the hydride−acetylide is formed in the presence of the d^8 planar fragment $[Cl(PR_3)_2Rh]^+$. However, an ad hoc theoretical study[4b] showed that the straightforward 1,3-H shift cannot be pursued. More probably, the vinylidene species forms through a bimolecular mechanism where the hydrogen atom coordinated to one metal is transferred to the C_β acetylide atom of a second, properly oriented, complex molecule. The coordinated hydrogen atom in the latter follows the parallel path in the opposite direction. Although novel and interesting, the bimolecular mechanism cannot be invoked in all cases involving the hydride−acetylide species. We refer in particular to the chemistry supported by the ancillary d^8 metal fragment $[(pp_3)Co]^+$ [pp_3 = $P(CH_2CH_2PPh_2)_3$][6] or by the d^6 metal fragment $[Cp^*(dippe)_2Ru]^+$ dippe = $iPr_2PCH_2CH_2PiPr_2$].[7] Kinetic and spectroscopic studies of these species provide evidence that the reaction leading to vinylidene is first-order unimolecular. Most probably, the bulkiness of the phenyl substituents in pp_3 makes docking of two molecules difficult. Finally, the hydride−acetylide complexes $[(pp_3)CoH(C{\equiv}CR)]^+$ (the derivative with R = $SiMe_3$ could be structurally characterized since it is inert to further transformation[6]) generally undergo transformation into the most stable vinylidene complex, even in the solid state, i.e. simply upon warming the crystals. Mainly because of spatial constraints within the lattice, the unimolecular reaction implies minimal geometrical rearrangement. Thus, especially in the presence of a bulky acetylene substituent such as phenyl, it is unthinkable that the hydride−acetylide can undergo reversion to the π-adduct, and hence that the reaction proceeds through a 1,2-H shift. In any event, by disregarding the spatial constraints of the solid state, it is interesting to evaluate the barrier for the reverse C−H reductive elimination of the hydride−acetylide and, where possible, that for the conversion of the π-adduct into the final vinylidene complex.

In order to focus more intently on this point, and since the system reported by Bianchini et al.[6] {that involving the d^8 metal fragment $[(pp_3)Co]^+$} has never been theoretically investigated in detail, we have performed specific ab initio calculations (the MP2 level was selected to be consistent with the approach adopted in ref.[4b]). The same set of calculations has been carried out for the isoelectronic fragment $[(pp_3)Rh]^+$, which is reported to yield only the hydride−acetylide species.[8] The sufficiently satisfactory numerical results are reported herein. We also outline some important chemical implications using the qualitative language of Perturbation Theory. In fact, a pictorial MO analysis (EHMO method using the CACAO package[9]) allows the evolution of the MOs between structural key-points on the reaction coordinate, already indicated by the ab initio results, to be monitored. The two approaches are not inconsistent, so that ultimately the quantitative and qualitative theoretical inferences allow a good understanding of the system based on common chemical intuition.

Computational Details

EHMO Calculations

In MO calculations of the extended Hückel type,[10] a weighted-modified Wolfsberg−Helmholz formula[11] was used. Literature STO parameters were used for Co,[12] while standard values were used for the main group elements. The 3D drawings, correlation and interaction diagrams were generated using the program CACAO.[9]

Ab Initio Calculations

The ab initio calculations were performed with the Gaussian-94[13] program at the MP2 level (electron correlation by second-order Møller−Plesset perturbation) using the ECP (effective core potential) approximation for some atoms. Specifically, the 17-electron ECP of Hay and Wadt[14] was adopted by using the [3s3p2d]/(5s5p5d) and [3s3p2d]/(5s5p4d) basis functions for cobalt and rhodium, respectively. Moreover, in order to further reduce the computational burden, 10- and 2-electron ECPs were adopted for phosphorus and carbon atoms, respectively, by using the [2s2p]/(4s4p) basis set.[15] For the H atoms, the D95 set was adopted.[16] Single-point energy calculations on the optimized structures were carried out using the same effective core potential for the metal and the 6-31G* basis set[17] for the other atoms. Unless otherwise specified, we discuss energies at these highest basis sets. Finally, to test the reliability of the ECP approximation, the computations were repeated using the ECP only for the transition metal, while a 6−31G basis set was used for the remaining atoms. The differences are not substantial, as can be seen on inspection of the data in Table 1.

In all cases, the geometries of the stationary points were fully optimized at the MP2 level using the analytical gradient under the C_s symmetry constraint. The transition state structures were relaxed after introducing small perturbations to ensure that they were indeed associated with the corresponding reactants and products. In the complexes with independent PH_3 ligands, the true minima or the transition state points on the potential energy surface were detected by calculating the second energy derivative matrix. Only for one of the optimized structures containing the actual model of the ligand pp_3 (refer later to **3a** in Figure 1) were the frequencies calculated. Although one imaginary frequency was found (not unexpectedly in view of the imposed C_s symmetry, see the later discussion), the optimized structures were still considered acceptable from a chemical viewpoint.

Results and Discussion

Ab Initio Calculations: Modelling Strategies and Energetic Trends

The tripodal ligand pp_3 was first mimicked with four independent PH_3 molecules, as is a common practise in MO calculations. As a result, various isomers of the general for-

Table 1. Experimental and calculated distances and angles for Co^{I}-vinylidene cationic complexes

	Ligand pp_3				Four (PH_3) ligands		
	Expt. Struct.[a]	ECP-31G[b]	ECP-31G[b]	6-31G[b]	Expt. Struct.[c]	ECP-31G[b]	6-31G[b]
Symmetry	C_1	Cs	C_1	Cs	C_1	C_{2v}	C_{2v}
$Co-P_1$	2.185	2.16	2.16	2.14	2.252	2.30	2.33
$Co-P_2$	2.21	2.23	2.24	2.24	2.246	2.30	2.33
$Co-P_3$	2.20	2.11	2.11	2.11	2.214	2.14	2.15
$Co-P_4$	2.205	2.11	2.11	2.11	2.219	2.14	2.15
$Co-C_1$	1.71	1.67	1.67	1.67	1.728	1.68	1.68
$C1-C_2$	1.34	1.38	1.38	1.34		1.38	1.34
P_1-Co-P_2	87.0	90.41	90.43	90.06	109.58	99.64	97.78
P_1-Co-P_3	85.0	89.36	89.24	89.44	92.02	95.83	96.43
$P1-Co-P_4$	84.3	89.36	89.49	89.44	95.87	95.83	96.43
P_2-Co-P_3	108.8	102.35	103.18	102.44	95.58	95.83	96.42
P_2-Co-P_4	109.1	102.35	101.34	102.44	95.27	95.83	96.42
P_3-Co-P_4	140.0	155.28	155.45	155.10	163.60	161.88	160.40
P_1-Co-C_1	164.5	154.83	154.36	155.56	133.51	130.20	131.09
P_2-Co-C_1	107.5	114.76	115.20	114.38	116.37	130.17	131.13
P_3-Co-C_1	91.5	85.37	85.45	85.46	81.61	80.94	80.19
P_4-Co-C_1	89.0	85.37	85.17	85.46	82.58	80.94	80.19
$Co-C_1-C_2$	168.5	177.16	177.26	177.20		180.00	180.00

[a] Average values of the two complex cations $[(pp_3)Co-C{=}CHPh]^+$ reported in ref.[6] – [b] For metal atoms, the effective core potential (ECP) of Hay and Wadt was chosen. – [c] Values for the complex $[(PH_3)_4Co-CO]^+$ reported in ref.[18]

mula $[(PH_3)_4Co(C_2H_2)]^+$ could be optimized, although the geometries were not fully consistent with the structural data available for $[(pp_3)Co(C_2HR)]^+$.[6] Data are available for the hydride–acetylide species with R = $SiMe_3$ (**III**), which is sufficiently stable for X-ray analysis. Conversely, the vinylidene isomer is most easily obtained for R = phenyl (**IV**). In this case, the transformation starting from the corresponding hydride–acetylide complex proceeds even in the solid state, simply upon warming the crystals.

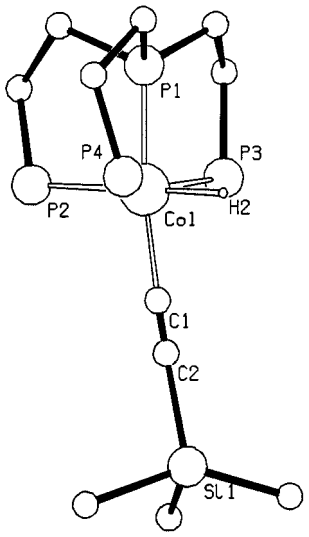

III

The most obvious difference between **III** and **IV** is the shape of the L_4M ancillary fragment. While the skeleton of $(pp_3)Co$ is approximately trigonal-pyramidal in **III**, a butterfly shape (*pseudo*-C_{2v} symmetry) is observed in the hydride–acetylide complex **IV**. Because of the constraints due to the ethylenic chains, the interconversion can only occur through the pathway **V**. Thus, all of the P_c-M-P_t angles remain close to 90°, while one of the P_t-M-P_t angles

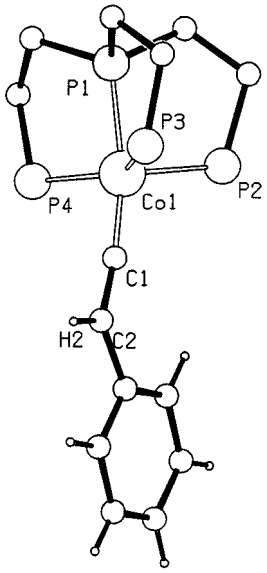

IV

opens out towards 180°. The latter angle, α, can be considered as a governing parameter in this type of reactivity as promoted by $(pp_3)M$ fragments (vide infra).

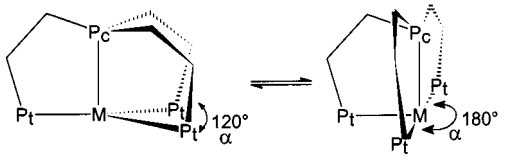

V

As mentioned above, the inadequacy of $(PH_3)_4Co$ as an ancillary fragment is evident as some parameters diverge significantly from the experimental values. In particular, one of the angles P_c-Co-P_t, which are all close to 90° in the actual fragment $(pp_3)Co$, is found to be as large as

145.5° at the transition state along the pathway **a** (see **II**). Another aspect is that the free PH_3 ligands are clearly subject to steric hindrance. Thus, in the optimized pseudo-octahedral hydride−acetylide complex, the two *trans*-axial phosphane ligands are not perfectly linear but are bent away from the equatorial ligands in order to avoid short contacts (angle of 157.7°). The same feature has been observed in the structure of $[(PH_3)_4CoCO]$[18] (the structural parameters of the latter are reported in Table 1), which would, however, be unattainable with the ligand pp_3. In fact, no vinylidene complex with four independent phosphane ligands has ever been reported. Indirectly, this may suggest that the variations of the stereochemistry about the metal atom impose a subtle orbital control on the acetylene−vinylidene transformation. Thus, we then focused on the results of MP2 calculations where the ligand pp_3 was mimicked with the model $P(CH_2CH_2PH_2)_3$ (terminal hydrogen atoms in place of the phenyl substituents). The need for the actual tripodal ligands in ab initio calculations has recently been stressed by other authors.[19]

To reduce the computational burden and to exploit at least one symmetry element, the skeletal atoms of one $P_cCH_2CH_2P_t$ arm as well as the cobalt atom were forced to be planar, thus ignoring the propensity of the aliphatic chains to be chiral. Indeed, use of this C_s approximation for the models **1a**, **2a**, and **3a** (see Figure 1) did not dramatically affect the results.[20] Moreover, comparison with the experimental cobalt structures **III** and **IV** was sufficiently satisfactory (see Table 1).

In the vinylidene model **3a**, the $C{=}CH_2$ group is not perfectly *trans* to the central P_1 atom (the calculated $C_\alpha{-}Co{-}P_1$ angle is 154.8° cf. the value of 164.5° found in the experimental structure). The P_4Co unit in the hydride−acetylide model **2a** even diverges significantly from the pseudo-C_{2v} symmetry found for the $(PH_3)_4Co$ model. In particular, the angle α defined in **V** is rather small (158.8°), in spite of the presence of the H ligand in its bisector. The corresponding angle in **3a**, $P_3{-}Co{-}P_4$, does not vary significantly (155.3°), although the experimental value is smaller (140.0°).

The transition states **4a** and **5a** were determined using the appropriate Gaussian-94 algorithm (STQN[21]), which exploits structural knowledge of both the reactant and the product, namely the pairs **1a**−**2a** and **2a**−**3a**, respectively. Furthermore, since our present computational capabilities are limited, no attempt was made to confirm that the detected transition states (**4a** and **5a**) were indeed the correct ones through calculation of the frequencies. Nevertheless, the latter species do not only exhibit a satisfactorily correct geometry for the P_4Co chromophore, but also appear chemically realistic. In particular, **4a** corresponds to the expected *agostic*-type adduct, which precedes the oxidative addition, while **5a** sheds new light on the mechanism leading to the formation of the vinylidene product. In fact, this structure differs somewhat from that calculated by Morokuma′s group[4a] for the process supported by the fragment $[Cl_2(PH_3)_2Ru]$, for which the formation of a hydride−acetylide species was ruled out. In the latter, the transferring

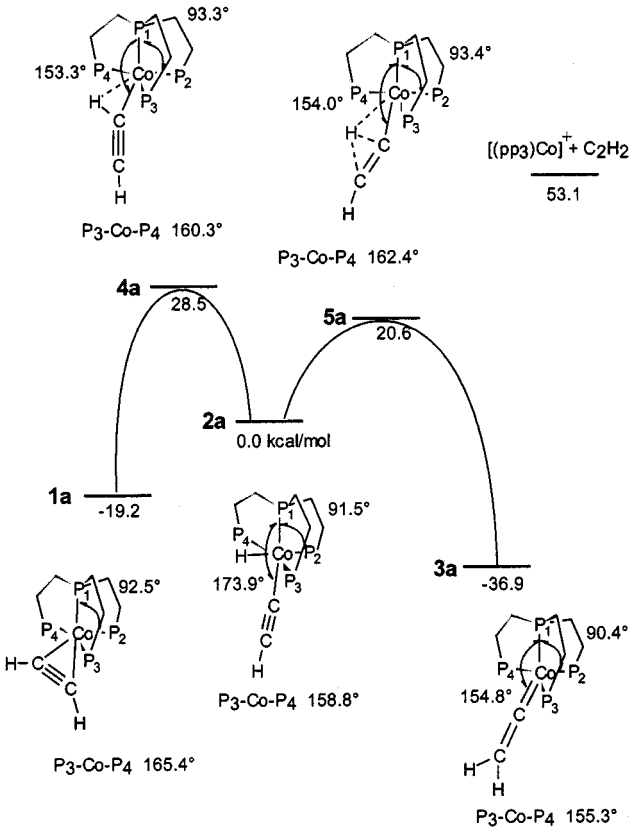

Figure 1. Optimized structures and relative energetics (MP2 level) along the pathway of interconversion between acetylene and vinylidene as promoted by the fragment $[P(CH_2CH_2PH_2)_3Co]^+$

hydrogen is strongly linked to the C_α atom (1.13 Å) and is far removed from C_β. Conversely, in **5a** a quasi-symmetrical bridging mode of hydrogen over the C−C linkage is observed. This is similar to the transition state detected[4b] for the unimolecular conversion of $[Cl(PH_3)_2RhH(C{\equiv}CH)]$ into $[Cl(PH_3)_2Rh(C{=}CH_2)]$, a process which is, however, disfavored with respect to the bimolecular one.

Before commenting on the energetics involved and on their evaluation in relation to the mechanism of the cobalt-induced reactions, we also present the parallel results (Figure 2) calculated using the fragment $[(pp_3)Rh]^+$. The latter is experimentally known to prevent the ultimate formation of the vinylidene complex[8b] starting from the hydride−acetylide isomer. Indeed, this species is the only stable product of the reaction of acetylene at the metal.

The structural keypoints are essentially similar to those in Figure 1. Perhaps the most obvious difference concerns the vinylidene structure **3b**, where the angle $P_1{-}Rh{-}C$ is smaller than that in **3a** (143.7° vs. 154.8°). This would seem to reveal a tendency of the $C{=}CH_2$ group to become better aligned with the bisector of the angle $P_1{-}M{-}P_2$, thus approaching more closely the behavior of the free phosphane model. In the latter C_{2v} structure, the $P_1{-}Co{-}C$ angle is as small as 130.2°.

Comparison of the data in Figures 1−2 and Table 1 reveals that the vinylidene species is most stabilized in the cobalt complex ($\Delta E = -36.9$ kcal/mol for **3a**) and that the

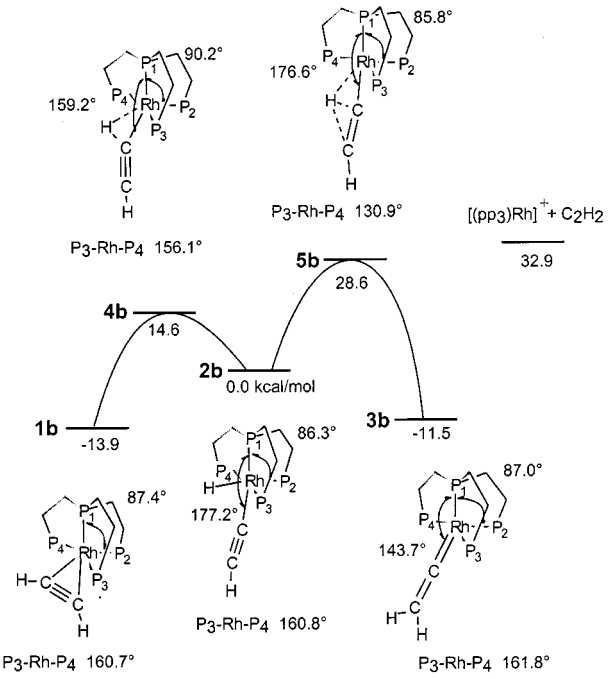

Figure 2. Optimized structures and relative energetics (MP2 level) along the pathway of interconversion between acetylene and vinylidene as promoted by the fragment $[P(CH_2CH_2PH_2)_3Rh]^+$

barrier associated with its formation is not large (20.6 kcal/mol for **5a**). In comparison, the rhodium vinylidene **3b** is much less stabilized (only −11.5 kcal/mol) and its associated barrier is larger (28.6 kcal/mol for **5b**). Furthermore, it is remarkable for rhodium that the barrier to reversion to the starting π-adduct is only 14.6 kcal/mol, practically half the magnitude of that calculated for cobalt. Concerning the transition states **4** in the direction of formation of the hydride−acetylide, the C−H oxidative addition of acetylene has a critically large value for cobalt (over 40 kcal/mol). Nevertheless, this does not seem unreasonable considering that the experimental reaction requires heating.[6] It must also be mentioned that, while the transition states of type **5**, i.e. between hydride−acetylide and vinylidene complexes (path *b* in **II**) have easily been detected, location of the transition states of type **4**, i.e. those involving an *agostic* interaction (path *a* in **II**), has proved much more time-consuming. The latter could only be determined through a trial and error approach based on small geometric modifications of the π-acetylene complexes **1**. Finally, like other authors before us,[4] we have not been able to detect a transition state between π-acetylene **1** and vinylidene **3** (path *c* in **II**). Only the most recent calculations[4c] on the system based on the fragment F_4W have led to the location of the corresponding transition state, following a systematic search after removing any possible symmetry.

In summary, the C−H oxidative addition process yielding complex **2** from **1** has been shown to be much more facilitated by rhodium than by cobalt, as is also the case for the reverse reductive elimination process. Moreover, the calculations have confirmed what was experimentally known, i.e. that the transformation **2** → **3** is quite straightforward with cobalt (it occurs in the solid state), but is impossible with rhodium. Besides having a larger associated barrier, the rhodium vinylidene complex does not seem to possess the necessary stability to be a terminal product. Another interesting numerical result, which confirms the better propensity of the cobalt fragment to function as an activator of acetylene, is contained in Figures 1 and 2. The energy of the separated fragments is distinctly higher for cobalt than for rhodium (53.1 vs. 32.9 kcal/mol), thus confirming the greater propensity of cobalt to promote this chemistry.

Considerations from the Viewpoint of Qualitative MO Theory

In this section, we mainly try to develop interpretational arguments concerning the second part of the pathway, leading from hydride−acetylide to vinylidene. The Hoffmann group, besides addressing the overall process of alkyne activation,[3] has also dedicated much attention to step of the C−H activation relative to the parallel dichotomy between η^2-ethylene and vinyl−hydride complexes.[22]

An intriguing aspect of the H migration ensuing from the hydride−acetylene adduct is the nature of the migrating hydrogen itself, i.e. whether it has proton or hydride character. Bianchini et al.[6] have reported that the vinylidene complex $[(pp_3)Co(C{=}CRH)]^+$ may be obtained not only through tautomerization of the alkyne HC≡CR by the 16-electron fragment $[(pp_3)Co]^+$, but also through straightforward protonation of the 18-electron acetylide complex $[(pp_3)Co(C{\equiv}CR)]$. More recently, de los Ríos et al.[7] reported that the isomerization of the hydride−acetylide species $[Cp^*RuH(C{\equiv}CR)(dippe)]^+$ to vinylidene is inhibited by strong acids such as HBF_4. While these facts are indicative of the strongly nucleophilic character of the acetylide C_β atom in the 18-electron complexes, it is difficult to envisage a proton migrating all the way from the metal atom.

In pseudo-octahedral Co^{III} complexes of type **III**, the orbital of the H ligand is energetically well below the σ hybrid of the fragment ML_5, **VI**. The latter, mainly z^2 in character, is destabilized by an antibonding interaction with the *trans*-axial phosphane, which promotes hybridization with the higher *s* and *pz* orbitals. In agreement with chemical intuition, the hydride is a donor.

In principle, a cooperating base could extract the H ligand as a proton and transfer it elsewhere. This is also the essence of the bimolecular mechanism proposed by Morokuma et al.,[4a] where the metal of the second molecule itself acts as the extracting base. In the present case, however, the process, which also occurs in the solid state, is not assisted by any external agent, nor is it feasible for two highly hindered complex molecules to get sufficiently close to one another. In the crystal, it is also hard to imagine a structural rearrangement that could bring the nucleophilic C_β atom sufficiently near the metal to extract the proton. Moreover,

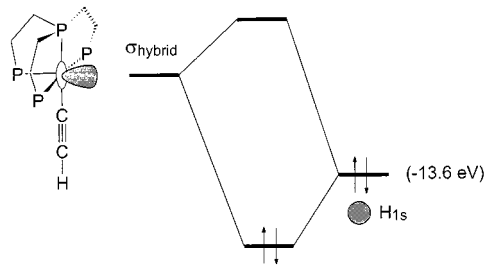

VI

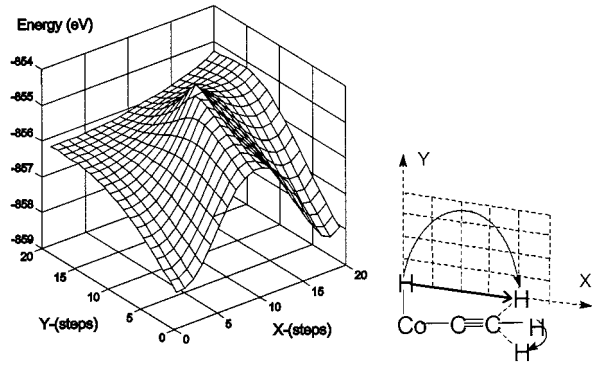

Figure 3. Potential energy surface (PES) calculated (EHMO method) on the small two-dimensional grid; the origin of the latter corresponds to the complex $[(PH_3)_4CoH(C{\equiv}CH)]^+$, with the *y* coordinate corresponding to the progressive separation of the H atom from the linear grouping $Co-C_\alpha-C_\beta$; the non-orthogonal *x* axis, which accounts for the non-equivalence of the $Co-H$ and $C_\beta-H$ bond lengths, describes the H shifting along the same grouping; irrespective of the *y* value, the $C_\alpha-C_\beta-H$ angle begins to bend as soon as the vectors $Co-C_\alpha-C_\beta$ and $C_\beta-H$ become orthogonal

if H^+ could separate from M^-, there would remain a hole in the overall MO picture (i.e. the empty H_{1s} orbital would lie below the occupied metal d block, including the high-lying metal σ lone pair). Thus, at least in the early stages of $M-H$ dissociation, the bonding electron pair is more reasonably assigned to the H atom. In any event, even though a net separation of charges may not be realistic, the extreme viewpoints of migration of a proton or a hydride are helpful in delineating the actual situation.

Although the ab initio calculations indicate that at the transition state the migrating H atom is close-bridging between the C_α and C_β atoms, a migration out of the domains of the latter atoms cannot, in principle, be excluded. However, since this would correspond to the heterolysis of two charged species, unassisted by any solvent, no satisfactory response can be expected based on ab initio theory. Indeed, as the calculations are based on a gaseous system, the attractive electrostatic interactions would overwhelm any opposing repulsive effect. An indirect confirmation of the possible coexistence of hydride and the species $[(pp_3)Co(C{\equiv}CR)]^{2+}$ might perhaps be provided by a straightforward optimization of the latter. Experimentally, the stability of the 16-electron pentacoordinated complex is confirmed by several crystal structures involving d^6 metals, mainly of the second and third transition rows,[23] and further support is provided by theoretical studies, including ab initio calculations with a proper orbital rationale.[24] In contrast, we are not aware of any stable Co^{III} species having a 16-electron count. Moreover, all our attempts to reach convergence for the model $[(pp_3)Co(C{\equiv}CR)]^{2+}$ (at the MP2 level) were unsuccessful because of large oscillations about the energy minimum. Thus, not even an indirect proof of the M^+-H^- heterolysis could be obtained.

While the existence of the *ion pair* cannot readily be demonstrated at the ab initio level, the extended Hückel method neglects the electrostatic term. Thus, in order to compare the MO behavior at any limiting geometrical situation, Figure 3 shows the EHMO 3D potential energy surface (PES). The latter is constructed on the two-dimensional grid appearing at the lower right-hand side of the figure, where the axes correspond to the increasing $M-H$ separation (positive *y*) and to the shifting of the H atom along the $M-C_\alpha-C_\beta-R$ direction (positive *x*). The origin corresponds to the hydride−acetylide Co^{III} complex itself.

In the early stages, the $[(pp_3)Co(C{\equiv}CR)]^{2+}$ fragment is kept in a fixed geometry and, in particular, the critical angle α, P_3-Co-P_4 (see **V**), is fixed at 150°. On approaching the final vinylidene product, narrowing of the terminal $C_\alpha-C_\beta-R$ angle is allowed. Interestingly, on the side of the surface facing the observer, there is a barrier which reproduces, at least geometrically, the transition state **5a** obtained by MP2 calculations (at EHMO level the barrier is large, ca. 50 kcal/mol). On the other hand, on descending the *y* axis (on the left side), the energetic cost of the $Co-H$ cleavage remains comparable so that, in principle, the hydride could migrate isolated behind the highest peak of the PES until it falls towards the C_β atom.

Some sound chemical inferences may be gained from the Walsh diagrams shown in Figure 4, which refer to alternative pathways indicated by the arrows in the small grid of Figure 3.

In the diagram on the far left, complete $M-H$ *heterolysis* is followed by coupling of the hydride with the C_β atom. The HOMO−LUMO gap, fairly large and constant over the central region, becomes small (ca. 0.5 eV) at some later point, so that even a change of the ground state can be hypothesized (singlet → triplet). Conversely, for the *close-contact* H migration, the gap is never smaller than 2 eV and none of the latter complications can be expected.

As the H atom moves parallel to the $Co-C_\alpha-C_\beta$ direction, the effects on some important MOs may be generalized, even if their extent depends on the initial $M-H$ separation. Figure 5 focuses on the behavior of only four levels. Starting from the left, these are the pair of occupied/empty σ and σ^*_{M-H} MOs of the hydride−acetylide species (see **VI**), and the pair of occupied/empty MOs corresponding to the in-plane π and π* levels of the acetylide.

As the H_{1s} orbital moves away from the direction of the metal σ hybrid, their overlap diminishes so that the σ^*_{M-H} level (LUMO) is stabilized. For an already long $M-H$ distance, this effect cannot be large as the LUMO energy would quickly reach the constant minimum, essentially the energy of the metal σ hybrid itself. In the left-hand diagram

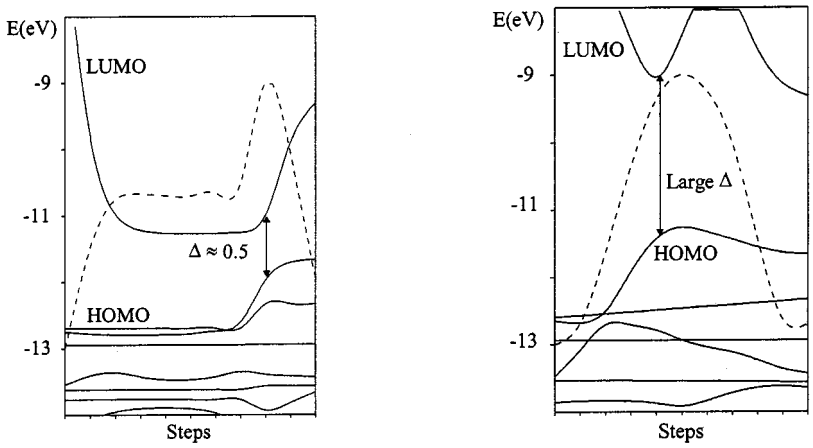

Figure 4. Walsh diagrams (EHMO calculations) relating to the two pathways indicated by the curved and straight arrows in the small grid of Figure 3, respectively; the far left-hand diagram corresponds to a H atom that migrates while physically separated from the rest of the molecule; the far right-hand diagram goes through the bridging H mode, corresponding to the ab initio transition state **5a** as depicted in Figure 1; the dashed lines refer to the total energy, for which each increment on the *y* axis corresponds to 0.6 eV

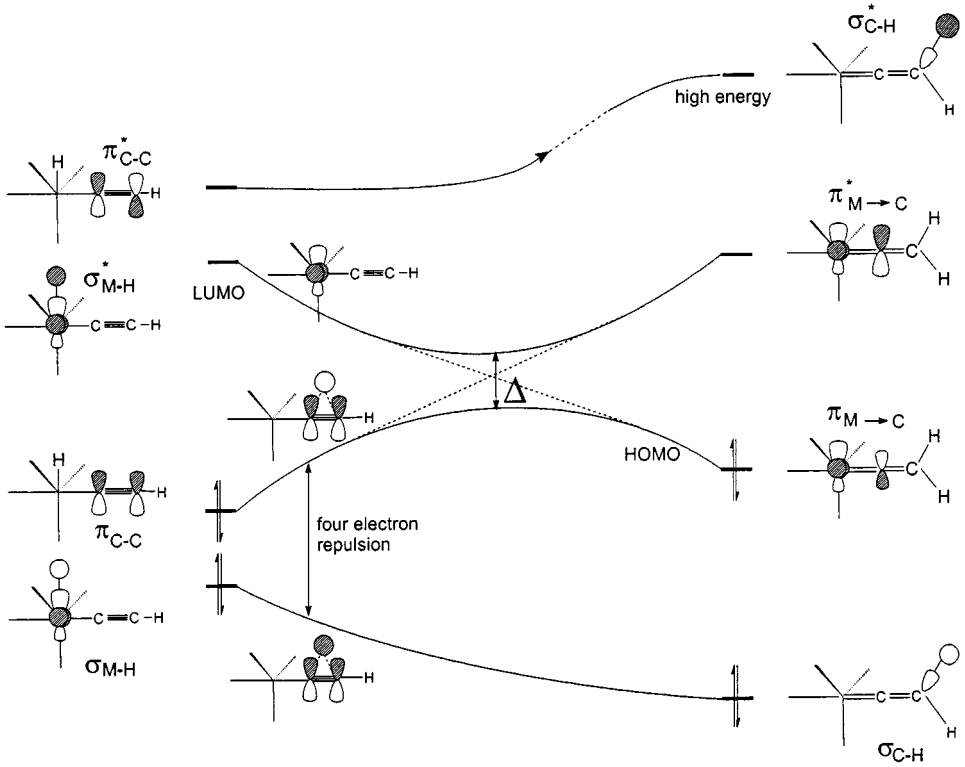

Figure 5. Schematic evolution of selected *in-plane* frontier MOs upon shifting of the H atom (initially the hydride ligand bound to the metal) along the linear grouping $Co-C_\alpha-C_\beta$; a four-electron repulsion between the hydride and one π-acetylene electron pair causes the destabilization of the HOMO, and hence is the origin of the barrier; the effect is subsequently counterbalanced by an interplay of orbital mixings, which brings metal character to the HOMO x^2-y^2 and involvement in some sort of back-donation

of Figure 4, the LUMO takes on C−H σ* character in the final steps and rises again until all of the character is transferred into high-lying MOs. Conversely, when the hydrogen atom is closer to the C−C linkage (right-hand diagram in Figure 4), the LUMO destabilizes soon after the initial stabilization. At the same time, a low-lying occupied level increases in energy and becomes the new HOMO.

Essentially, the origin of the *avoided* HOMO−LUMO crossing, highlighted in Figure 5, can be described as follows. On moving away from the metal, H_{1s} begins to interact with the π_{C-C} bonding MO, giving rise to diverging *in-phase* and *out-of-phase* combinations (the latter being the HOMO, as shown in Figure 5). At least initially, due to the shortness of the C≡C triple bond, π^*_{C-C} is too high to mix into the HOMO so as to alter the depicted repulsion between H_{1s} and π_{C-C}-based orbitals. Subsequently, the intermixing between all of the levels of Figure 5 (isosymmetric) becomes more significant. Thus, the descending LUMO (σ^*_{M-H}) and the rising HOMO evidently undergo an *avoided crossing*, which involves π^*_{C-C} as well. By virtue of

the latter, the pπ contribution from C_β disappears from both levels, which acquire a sort of π and π* character relative to $M-C_\alpha$ (see below). As mentioned above, the $C_\beta-H$ σ* character is only temporarily observed in the LUMO and is quickly transferred to higher levels.

Ultimately, the HOMO is largely centered on the metal and it can be assumed that its formal reduction has occurred, involving the electrons formerly on the hydride ligand. More precisely, the x^2-y^2 component, although not strictly a dπ orbital, can make some back-donation into the $C_\alpha p_\pi$ orbital through its most hybridized lobe, so that the M=C=C bonding formulation is reasonable. Moreover, it can be shown that the nature and extent of the back-donation are subtly governed by the geometrical flexibility of the pp_3 ligand (vide infra).

Recall that the vinylidene complex containing four independent PH_3 ligands was optimized with C_{2v} symmetry, as was the fragment $[(PH_3)_4Co]^+$. The latter of the type d^8-L_4M and with butterfly shape is characterized by an equatorial, occupied d_ϕ hybrid,[25] which is most suitable for back-donation. Significantly, in this complex, the grouping $C=CH_2$ is perfectly aligned with the bisector of the two angles P_1-Co-P_2 and P_3-Co-P_4. The same picture does not quite apply to the fragment $[(pp_3)Co]^+$, which is at most C_s and is somewhat reminiscent of threefold symmetry (Figure 1). Under these circumstances, the coordinated $C=CH_2$ grouping remains close to one apical position of the trigonal bipyramid (*trans* to P_1), with the angle P_1-Co-C_α deviating from linearity by only 15° (experiment[6]) or 25.2° (MP2 structure **3a** in Figure 1). As already discussed, the angle P_1-Co-P_2 is almost fixed at 90°, while the angle P_3-Co-P_4 (α in **V**) is free to open from 120° (up to 140° in the experimental structure and even more so in the optimized structure **3a**, i.e. 155.3°).

The angle P_3-Co-P_4 plays a major role in governing the dπ back-donation capabilities of d^8-L_4M fragments. Figure 6 shows the evolution of the frontier MOs of the trigonal-pyramidal fragment $[(PH_3)_4Co]^+$ (left side) on widening one equatorial P−Co−P angle over the range 120−180°. At the right-hand side, the fragment has a butterfly shape with the typical FMOs ($t_{2g} + d_\phi + \sigma_{hybrid}$).[25]

At the trigonal-pyramidal stage, the metal orbitals consist of two *e* sets (*xz*/*yz* orbitals, unperturbed, and *xy*/x^2-y^2 orbitals partially destabilized by the equatorial ligands) and of a higher a_1 level (σ_{hybrid}, largely z^2 in character and destabilized by the axial ligand). On widening of the angle, 1*e* and a_1 remain unaffected, but the 2*e* components diverge. In fact, the two equatorial ligands slip off two consecutive lobes of *xy* and progressively point more towards the nodes of the orbital, while an opposite trend is seen for x^2-y^2. Ultimately, *xy* becomes equivalent to *xz* and *yz* ("octahedral" t_{2g} set), while x^2-y^2 is so destabilized that its crossing with the higher z^2 (a_1) is attempted but *avoided* because of the equal symmetry (*a′* in C_s). The resultants of a z^2/x^2-y^2 mixing, usually difficult to visualize, are well illustrated by the CACAO pictures[9] in Figure 6. Thus, the former a_1 level reorientates the main σ lobe up to 45° in the plane *xz* and maintains the original σ character, albeit with

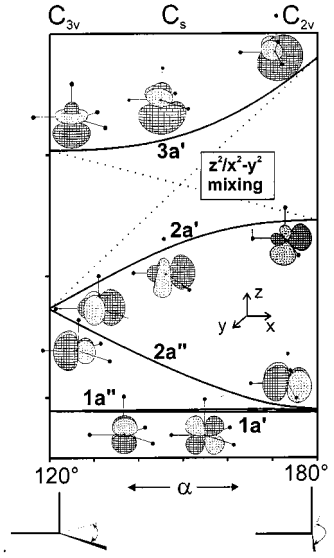

Figure 6. Evolution of the metal d orbitals during the interconversion of an L_4M metal fragment from trigonal-pyramidal to butterfly geometry, the unique governing factor being the opening of one equatorial L−M−L angle; avoided crossing between x^2-y^2 and z^2 slowly develops d_ϕ character at the former orbital, which is occupied in the d^8 configuration

reduced d orbital contribution. At the same time, the mixing transforms the most extended lobes of the somewhat hybridized z^2 and x^2-y^2 orbitals into a new orbital with progressively greater dπ character. At α = 180°, the well known d_ϕ hybrid typical of the L_4M fragments with butterfly shape is observed.[25] The ethylenic chains in the fragment $[(pp_3)Co]^+$ are resistant to full P−Co−P opening, so that an intermediate geometry can be stabilized as soon as the d_ϕ character is sufficient to allow back-donation into the vinylidene unit. This is most likely the key factor in interpreting the influence of the geometry of the ancillary ligand on the stability of the vinylidene complex.

Concluding Remarks

The experimental data and the present ab initio results indicate that, at least for the system $(pp_3)Co^I$, the hydride−acetylide species is the key basic intermediate en route to vinylidene. The essential qualitative arguments are shown schematically in Figure 7. The acetylene molecule adds to the d^8 metal through donation of its π bonding electron pairs into the acceptor σ hybrid orbital typical of the trigonal-pyramidal fragments. The metal bears a lone pair based on the occupied x^2-y^2 orbital, which is relatively high in energy. On opening of one P−M−P angle (α, see **V**), the metal develops the necessary d_ϕ character to trigger C−H oxidative addition (see Figure 6) and the pseudo-octahedral hydride−acetylide complex is formed.

Formally, the hydrogen ligand abstracts the lone pair from the metal so that a total of 12 valence electrons is consistently assigned to the whole grouping $H^- + CCH^-$. As soon as the hydride falls away from the position of maximum overlap with the σ metal hybrid, its electrons are re-

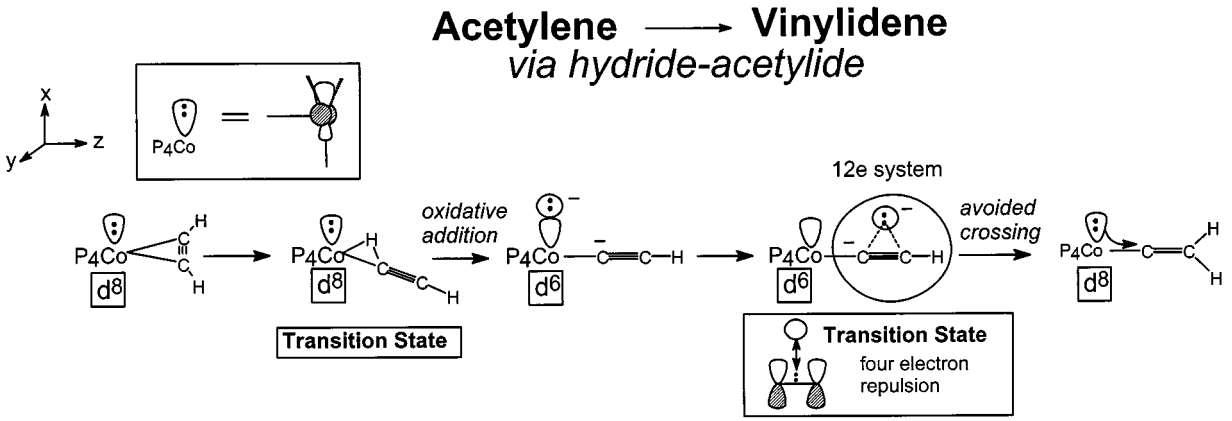

Figure 7. Structural highlights for the 1,3-shifts promoted by d^8 metal fragments; along this pathway, oxidative addition and reductive elimination of the metal involve a suitably modified orbital (originally x^2-y^2)

pelled by the electron cloud of the coplanar C−C π bond, as indicated in Figure 5. The four-electron repulsion is maximized at some point where the hydrogen bonds the two carbon atoms (transition state). The barrier is directly related to the destabilization of the HOMO, and the trend is inverted by an *avoided crossing mechanism.* By virtue of the latter, the hydride electron pair is returned to a metal orbital. This is essentially x^2-y^2, which characterizes the descending LUMO and ultimately concentrates into the HOMO. The final step on the pathway corresponds to the simple protonation of the C_β atom of the 18-electron acetylide complex, which occurs easily.[6]

At the transition state, the C_α−H and C_β−H distances are critically long, and are likely to limit the effects of the aforementioned four-electron repulsion. The calculated MP2 values are 1.32 and 1.48 Å, respectively. At longer C−H bridging distances, the energetics of the system would go steeply uphill toward the highest peak of the EHMO PES shown in Figure 3. Alternatively, the system might go around the peak by first elongating the M−H distance. In this case, the barrier would be essentially the energy of the M−H bond, which is too high. In fact, this is estimated to be no lower than 50 kcal/mol and significantly larger for second- and third-row transition metals.[26] Most probably because of the latter reason, the rhodium system stabilizes the hydrido−acetylide species and the barrier to vinylidene formation is distinctly higher than in the case of cobalt.

Even though the EHMO method neglects the important electrostatic component when charges are separated, it reveals an orbital drawback to the heterolysis. Namely, a small HOMO−LUMO gap along the pathway (left-hand diagram of Figure 4) would imply a necessity for a change in the ground state. If complete M−H heterolysis appears improbable, the hydrogen must start its migration as a hydride. When the C_β atom bears too great a negative charge, as is the case when it is bound to an electropositive silyl substituent, the migration may be inhibited and the hydride−acetylide species is stabilized.[6]

The general reactivity studied here has already received much theoretical attention. Despite this, no generalization of the results can yet be made. In the present study, we have not only performed ab initio calculations on a system which follows possibly unique pathways, but we have also offered some interpretations by exploiting the concepts of perturbation theory as well as by applying chemical intuition. From a quantitative point of view, it has become apparent that sufficiently good results are only obtainable with the most realistic model (use of the pp_3 ligand). At the same time, monitoring of the MO behavior along the reaction pathways has helped to resolve some major chemical ambiguities.

Acknowledgments

E. P.-C. is grateful to the Spanish Ministerio de Educacion y Cultura for a Postdoctoral grant. Financial support from EC contract ERBIC15CT-960746 is gratefully acknowledged. We thank the "Area della Ricerca CNR di Firenze" (in particular, Dr. Alberto Tronconi and Mr. Stefano Cerreti) for the providing computing time and facilities.

[1] K. M. Ervin, J. Ho, W. C. Lineberger, *J. Chem. Phys.* **1989**, *91*, 5974−5992.
[2] W.-C. Chen, C.-H. Yu, *Chem. Phys. Lett.* **1997**, *277*, 245−251 and references therein.
[3] J. Silvestre, R. Hoffmann, *Helv. Chim. Acta* **1985**, *68*, 1461−1506.
[4] [4a] Y. Wakatsuki, N. Koga, H. Yamazaki, K. Morokuma, *J. Am. Chem. Soc.* **1994**, *116*, 8105−8111. − [4b] Y. Wakatsuki, N. Koga, H. Werner, K. Morokuma, *J. Am. Chem. Soc.* **1997**, *119*, 360−366. − [4c] R. Stegmann, G. Frenking, *Organometallics* **1998**, *17*, 2089−2095.
[5] [5a] H. Werner, U. Brekau, *Z. Naturforsch.* **1989**, *44b*, 1438−1448. − [5b] T. Rappert, O. Nürnberg, N. Mahr, J. Wolf, H. Werner, *Organometallics* **1992**, *11*, 4156−4164. − [5c] H. Werner, M. Baum, D. Schneider, B. Windmüller, *Organometallics* **1994**, *13*, 1089−1089. − [5d] M. Oliván, E. Clot, O. Eisenstain, K. G. Caulton, *Organometallics* **1998**, *17*, 897−901.
[6] C. Bianchini, M. Peruzzini, A. Vacca, F. Zanobini, *Organometallics* **1991**, *10*, 3697−3707.
[7] I. de los Ríos, M. J. Tenorio, M. C. Puerta, P. Valerga, *J. Am. Chem. Soc.* **1997**, *119*, 6529−6538.
[8] [8a] C. Bianchini, A. Meli, M. Peruzzini, F. Zanobini, P. Zanello, *Organometallics* **1990**, *9*, 241−250. − [8b] C. Bianchini, D. Masi, A. Meli, M. Peruzzini, J. A. Ramirez, A. Vacca, F. Zanobini, P. Zanello, *Organometallics* **1989**, *8*, 2179−2189.
[9] C. Mealli, D. M. Proserpio, *J. Chem. Educ.* **1990**, *67*, 399−402.
[10] [10a] R. Hoffmann, W. N. Lipscomb, *J. Chem. Phys.* **1962**, *36*,

2872−2883. − [10b] R. Hoffmann, W. N. Lipscomb, *J. Chem. Phys.* **1962**, *37*, 3489−3493.
[11] J. H. Ammeter, H.-B. Bürgi, J. C. Thibeault, R. Hoffmann, *J. Am. Chem. Soc.* **1978**, *100*, 3686−3692.
[12] R. H. Summerville, R. Hoffmann, *J. Am. Chem. Soc.* **1976**, *98*, 7240−7254.
[13] M. J. Frisch, G. W. Trucks, H. B. Schlegel, P. M. W. Gill, B. G. Johnson, M. A. Robb, J. R. Cheeseman, T. A. Keith, G. A. Petersson, J. A. Montgomery, K. Raghavachari, M. A. Al-Laham, V. G. Zakrzewski, J. V. Ortiz, J. B. Foresman, J. Cioslowski, B. B. Stefanov, A. Nanayakkara, M. Challacombe, C. Y. Peng, P. Y. Ayala, W. Chen, M. W. Wong, J. L. Andres, E. S. Replogle, R. Gomperts, R. L. Martin, D. J. Fox, J. S. Binkley, D. J. Defrees, J. Baker, J. P. Stewart, M. Head-Gordon, C. Gonzalez, J. A. Pople, *Gaussian-94*, Gaussian Inc., Pittsburgh, PA, **1995**.
[14] P. J. Hay, W. R. Wadt, *J. Chem. Phys.* **1985**, *82*, 299−310.
[15] W. J. Stevens, H. Basch, M. Krauss, *J. Chem. Phys.* **1984**, *81*, 6026−6033.
[16] T. H. Dunning, P. J. Hay, *Modern Theoretical Chemistry* (Ed.: H. F. Schaefer III), Plenum, New York, **1976**, 1−28.
[17] [17a] P. C. Hariharan, J. A. Pople, *Theor. Chim. Acta* **1973**, *28*, 213−222. − [17b] M. M. Francl, W. J. Petro, W. J. Hehre, J. S. Binkley, M. S. Gordon, D. J. DeFree, J. A. Pople, *J. Chem. Phys.* **1982**, *77*, 3654.
[18] Y. Pérès, M. Dartiguenave, Y. Dartiguenave, *Organometallics* **1990**, *9*, 1041−1047.
[19] [19a] H. Jacobsen, H. Berke, *Chem. Eur. J.* **1997**, *3*, 881−886. − [19b] C. Bianchini, D. Masi, M. Peruzzini, M. Casarin, C. Maccato, G. A. Rizzi, *Inorg. Chem.* **1997**, *36*, 1061−1069.
[20] Frequencies were calculated for the most stable isomer **3b**. The only imaginary value has the largest components, indicating that the two C atoms in the mirror plane vibrate out of it, in opposite directions. In order to get an idea of the error introduced, complex **3b** was also optimized in C_1 symmetry. Since structural (Table 1) and energetic differences are small (< 2 kcal/mol), the C_s symmetry was retained for all of the key structures, including the transition states, **4a** and **5a**.
[21] C. Peng, H. B. Schlegel, *Isr. J. Chem.* **1993**, *33*, 449−454.
[22] J. Silvestre, M. J. Calhorda, R. Hoffmann, P. O. Stoutland, R. G. Bergaman, *Organometallics* **1986**, *5*, 1841−1851.
[23] [23a] C. R. S. M. Hampton, I. R. Butler, W. R. Cullen, B. R. Jones, J.-P. Charland, J. Simpson, *Inorg. Chem.* **1992**, *31*, 5509−5520. − [23b] R. L. Harlow, D. L. Thorn, R. T. Baker, N. L. Jones, *Inorg. Chem.* **1992**, *31*, 993−997. − [23c] M. D. Fryzuk, P. A. MacNeil, R. L. Massey, R. G. Ball, *J. Organomet. Chem.* **1989**, *368*, 231−247. − [23d] M. D. Fryzuk, P. A. MacNeil, R. G. Ball, *J. Am. Chem. Soc.* **1986**, *108*, 6414−6416. − [23e] H. Werner, A. Höhn, M. Dziallas, *Angew. Chem. Int. Ed. Engl.* **1986**, *12*, 1090−1092.
[24] [24a] M. Ogasawara, S. A. Macgregor, W. E. Streib, K. Folting, O. Eisenstein, K. G. Caulton, *J. Am. Chem. Soc.* **1995**, *117*, 8869−8870. − [24b] J. T. Poulton, M. P. Sigalas, K. Folting, W. E. Streib, O. Eisenstein, K. G. Coulton, *Inorg. Chem.* **1994**, *33*, 1476−1485.
[25] A. Albright, J. K. Burdett, M. H. Whangbo, *Orbital Interactions in Chemistry*, Wiley, New York, **1985**.
[26] F. Calderazzo. *Insertion Reactions: Principles and Applications*, Wiley, in preparation.

Received February 9, 1999
[I99032]